UDK 67:017:669.14.018.298:621.791.05
Professional article/Strokovni članek

ISSN 1580-2949
MTAEC9, 50(3)455(2016)

A COMPARISON OF AS-WELDED AND SIMULATED HEAT AFFECTED ZONE (HAZ) MICROSTRUCTURES

PRIMERJAVA MIKROSTRUKTURE TOPLOTNO VPLIVANEGA PODROČJA VARJENEGA IN SIMULIRANIH VZORCEV

Roman Celin[1], Jaka Burja[1], Gorazd Kosec[2]

[1]Institute of Metals and Technology, Lepi pot 11, 1000 Ljubljana, Slovenia
[2]Acroni d.o.o., Cesta Borisa Kidriča 44, 4270 Jesenice, Slovenia
roman.celin@imt.si

Prejem rokopisa – received: 2016-01-05; sprejem za objavo – accepted for publication: 2016-01-29

doi:10.17222/mit.2016.006

The high-strength steel grade S690QL and a filler welding wire Mn3Ni1CrMo were the materials chosen for welding a V-shaped butt weld. In order to prevent the weld's cold cracking, a multi-pass welding technique was applied. A metallographic investigation revealed microstructure variations in different areas of the weld's heat-affected zone. A reverse-engineering approach was used to test a dilatometer's capabilities to simulate different HAZ microstructures. Hollow steel-cylinder specimens were subjected to several weld thermal cycles in order to generate similar microstructures as in the real weld's HAZ. The microstructures of the as-welded and simulated heat-affected zone specimens were investigated. Good agreement was found between the dilatometer-simulated HAZ microstructures and those in a real HAZ weld.

Keywords: welded joint, microstructure, high-strength low-alloy steel, simulation, dilatometer, heat-affected zone

Visokotrdno jeklo S690QL in varilna žica Mn3Ni1CrMo kot dodatni material, sta bila uporabljena pri varjenju sočelnega V-spoja. Za preprečitev pokanja v hladnem je bila uporabljena tehnika večvarkovnega varjenja. Metalografska preiskava je odkrila različne mikrostrukture v različnih predelih toplotno vplivanega področja zvara. Za preizkus delovanja dilatometra je bil, za simulacijo mikrostruktur različnih področij toplotno vplivanega področja, uporabljen princip povratnega inženirstva. Različna mikrostruktura toplotno vplivanega področja je bila simulirana z izpostavitvijo votlih cilindričnih vzorcev različnim toplotnim ciklom. Opravljena je bila metalografska preiskava realnega zvarjenega spoja in simuliranih vzorcev. Primerjava rezultatov je pokazala dobro ujemanje simuliranih in realnih mikrostruktur.

Ključne besede: zavarjen spoj, mikrostruktura, visokotrdno jeklo, simulacija, dilatometer, toplotno vplivano področje

1 INTRODUCTION

The decision to use high-strength steel depends on a number of application requirements, such as thickness reduction, corrosion resistance, formability and weldability. The quenched and tempered low-alloy (QTLA) steels, usually containing less than 0.25 % carbon and less than 5 % alloying elements, are strengthened primarily by quenching and tempering to produce microstructures containing martensite and bainite.[1] S690QL is such a steel grade with high strength and toughness.[2]

Any common welding procedure can be used to join QTLA steels.[3] For any given steel, the welded joint's microstructures and the mechanical properties in the weld metal (WM) and the heat-affected zone (HAZ) are influenced mainly by the welding thermal cycle.

Due to the welding thermal cycle and the associated peak temperature, a change of the parent metal's microstructure and the mechanical properties happens in the HAZ. With increasing distance from the fusion line the peak temperature decreases, thus forming different microstructures. The width of the HAZ depends on the welding procedure, the thermal conditions and the physical properties of the parent metal.

Figure 1 shows a simplified presentation of different HAZ regions of a multi-pass welded joint. Weld pass 2 has a portion of HAZ that can be treated as a single weld pass and can be divided into four regions. These regions are defined by the peak temperature to which the region was exposed during the weld thermal cycle:[4,5]

- Coarse-grain region (CG HAZ) – material adjacent to the fusion line that reaches a peak temperature T_P above 1300 °C,
- Fine-grain region (FG HAZ) – T_P is lower, but still above A_{C3},
- Inter-critical region (IC HAZ) – T_P is between $A_{C1} < T_P < A_{C3}$,
- Sub-critical region (SC HAZ) – T_P is lower than A_{C1}.

However, the welding of thick steel components usually requires the application of a multi-pass welding procedure. In this case, the first pass (weld pass 1) HAZ regions are reheated to different peak temperatures during the second weld pass thermal cycle (weld pass 2). **Figure 1** also shows a simplified presentation of the different reheated first weld pass HAZ regions:[4,5]

- region 1: Super-critically reheated coarse-grain HAZ – SCR CG HAZ,

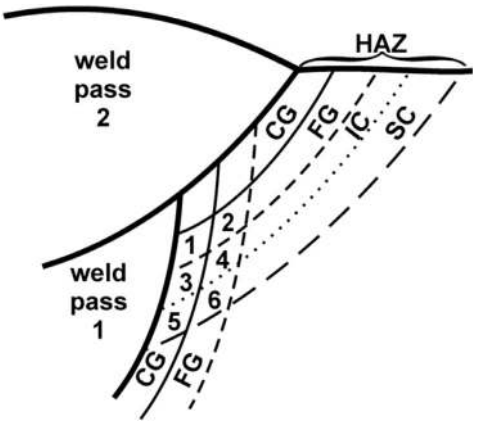

Figure 1: Simplified representation of the different regions of the HAZ
Slika 1: Poenostavljena predstavitev različnih območij toplotno vplivanega področja

- region 2: Inter-critically reheated coarse-grain HAZ – IR CG HAZ,
- region 3: Sub-critically reheated coarse-grain HAZ – SC CG HAZ,
- region 4: Super-critically reheated fine-grain HAZ – SCR FG HAZ,
- region 5: Inter-critically reheated fine-grain HAZ – IR FG HAZ,
- region 6: Sub-critically reheated fine-grain HAZ – SC FG HAZ.

In a real weld the HAZ regions are narrow in relation to the weld. To achieve regions of uniform microstructure suitable for investigations, weld simulators are used.[6-12] Usually, these weld thermal simulations are made in conjunction with weldability investigations to determine the proper welding parameters.

In the presented investigation a dilatometer with a controlled heating and cooling fixture was used to simulate the weld thermal cycles. The goal of the investigation was to test the dilatometer's capability to simulate the microstructures that correspond to the real weld's HAZ microstructures using a reverse-engineering approach.

2 EXPERIMENTAL PART

The chemical analysis of the Micral 690 sample with an ICP spectrometer was made prior to any further investigations. The determination of the welding parameters for the Micral 690 welding procedure was carried out by considering the EN 1011-2 recommendations, the steel manufacturer's specifications and the data from several papers.[13–16]

The two plates, with a thickness of 15 mm, a length of 500 mm, a width of 150 mm and a V-groove joint geometry, were welded with 8 passes using the sequence shown in **Figure 2**. A manual MAG welding procedure in a flat (PA) position was used. The filler material was grade Mn3Ni1CrMo welding wire with a diameter of

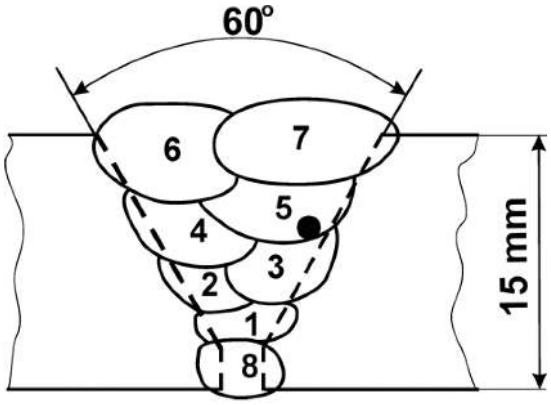

Figure 2: Sketch of the welded joint
Slika 2: Skica zavarjenega spoja

ϕ 1.2 mm, according to SIST EN ISO 16834[17]. The shielding gas used was a mixture M21 (82 % Ar + 18 % CO_2). The welding was carried by a skilled, certified welder and without preheating.

The welding current, voltage and time were recorded during the procedure. The weld pass 5 thermal cycle was recorded by dipping a type-S thermocouple (Pt Rh–Pt) directly into the weld's molten bead. The approximate position of the thermocouple is marked with a dot. Standard[18] non-destructive examinations and mechanical tests of the weld joint were also carried out and are described in a previous paper.[19]

Seven hollow, 10-mm-long cylinders with a 4-mm outer diameter and 1.5-mm inner diameter were machined from the weld's parent material (base metal) plate. Holes were bored in order to obtain a uniform heating and cooling of the sample during the thermal simulation.

The simulations were carried out with a TA instruments DIL805A/D quenching dilatometer in a vacuum atmosphere, with argon used as a coolant. Control of the thermal cycle was maintained via a type-S thermocouple that was spot welded directly onto the hollow cylinder sample.

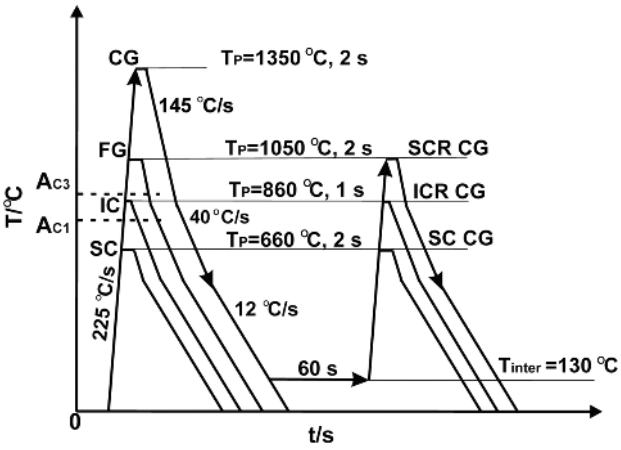

Figure 3: Schematic diagrams for the thermal cycle simulations
Slika 3: Diagrami za potek simulacij termičnih ciklov

Figure 3 shows schematic diagrams with the parameters for seven thermal cycle simulations used to generate the corresponding microstructure:

- single weld pass CG, FG, IC and SC regions of the HAZ,
- reheated weld pass SCR CG, IC CG, SC CG regions of the HAZ, as in **Figure 1**.

For the reheated simulated thermal cycles the same parameters were used as for the single-cycle simulation. The time–temperature dependence (**Figure 4**) recorded during weld pass 5 was used to determine the simulation heating rate, the peak temperatures, the holding times and the cooling rates.

During a single coarse-grain (CG) thermal cycle simulation the specimens' phase-transition temperatures A_{C1} and A_{C3} were recorded as well as the dilatation and temperature data from each simulation. The specimen was prepared by grinding and polishing with diamond paste, followed by a chemical etching with 5 % Nital.

Macro- and microscopic examinations[20–22] were performed using a light microscope (LM) to characterize the microstructures of the deposited weld metal, the heat-affected zone, the parent metal and the dilatometer-simulated hollow cylinder specimens of the parent metal.

A comparison between the as-welded and the dilatometer-simulated microstructures was carried out.

3 RESULTS AND DISCUSSION

The results of the parent metal's quantitative chemical analysis are presented in **Table 1**. The steel contains strong carbide-forming elements such as Nb, Mo, Cr and Ti, which ensure high strengths, even at elevated temperatures.

Table 1: Chemical composition of parent metal in mass fractions, *w*/%
Tabela 1: Kemična sestava jekla v masnih deležih, *w*/%

C	Si	Mn	P	S	Cr	Ni
0.164	0.29	0.72	0.006	0.001	0.54	0.20
Cu	Mo	Ti	Nb	Al	B	N
0.25	0.263	0.02	0.028	0.028	0.001	0.011

The applied welding parameters and the calculated welding speed and heat input were:

- weld length, 500 mm
- welding time, 132–422 s
- voltage, 21–22 V
- current, 100–165 A
- weld inter-pass temperature, 130 °C
- welding speed, 1.8–2.89 mm/s
- heat input, 1.03–1.63 kJ/mm

Lower-value welding parameters were applied for the root pass welding.

After the temperature–time data acquisition from the temperature-measurement instrument's memory card and data analysis for the welding pass 5, a cooling time $t_{8/5}$ of 7.6 s was determined and the peak temperature T_P was 1370 °C (**Figure 4**).

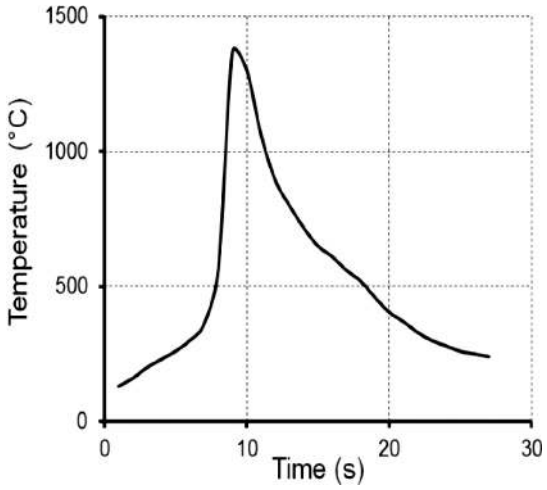

Figure 4: Weld pass 5 – recorded temperature – time dependence
Slika 4: Polnilni varek 5 – zabeležena odvisnost temperatura – čas

The shape of the cooling curve (**Figure 4**) is affected by the inter-pass temperature. Also, the weld's cooling time is prolonged due to the reduced temperature difference between the weld material and the surrounding parent metal.

Figure 5 shows the ICR CG HAZ recorded thermal cycle simulation with the temperature and the dilatation curve. From the dilatation data analysis of the phase transformation during the CG thermal cycle simulation the transition temperatures A_{C1} and A_{C3} were found to be 830 °C and 885 °C, respectively. During the rapid heating of steel, as in the case of welding, the phase-transformation temperatures are increased, the observed transformation temperatures A_{C1} and A_{C3} are well above equilibrium, i.e., about 710 °C and 785 °C respectively. The increase of the transformation temperatures is attributed to the diffusion process of the transformation from ferrite to austenite, which is time and temperature dependent. The dilatation curve in **Figure 5** clearly indicates that a transformation took place below 500 °C,

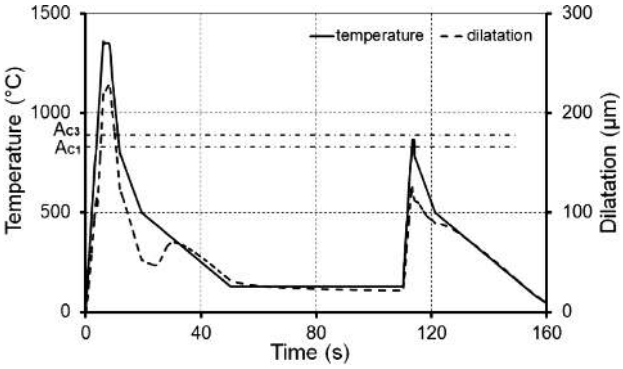

Figure 5: ICR CG HAZ thermal simulation with temperature-time and dilatation-time dependence
Slika 5: Potek temperature in raztezka v odvisnosti od časa pri simulaciji interktitičnega grobozrnatega TVP

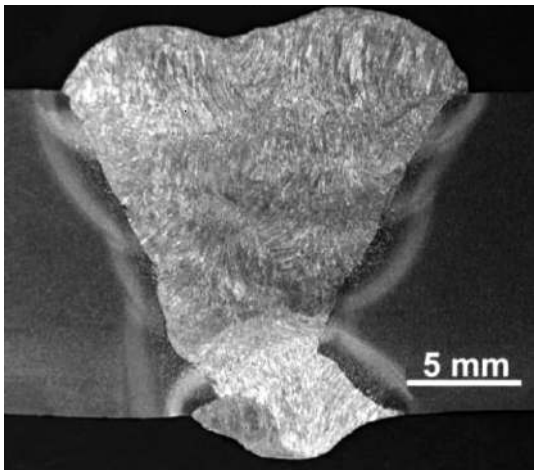

Figure 6: Welded joint macro section
Slika 6: Makroposnetek zavarjenega spoja

during the first cooling, and that another transformation took place during the second cooling, but it was not as intense as the first one, thus proving that the inter-critical temperature was indeed reached.

A good fit was found between the theoretical (**Figure 3**) and dilatometer-simulated thermal IR CG HAZ cycle (**Figure 5**). The heating rates, cooling rates, and holding times were very close to those programmed, with minor deviations due to the response of the dilatometer control and the regulation system. The first thermal cycle peak temperature was 1360 °C, with an inter-critical peak temperature of 866 °C.

Figure 6 shows the welded joint's macro section with each weld pass and the corresponding HAZ. Between subsequent weld passes an unaffected region of the coarse-grain HAZ microstructure can be distinguished. The reheated pockets of the CG HAZ regions are small and discontinuous, which makes their microstructure difficult to identify and investigate. During metallographic investigations the dimensions of the IR CG HAZ microstructure region were estimated to be 0.8 mm long and 0.3 mm wide.

Figure 7 shows the weld pass 5 HAZ area not affected by a subsequent weld pass thermal cycle. It is an area with a longitudinal microstructure transition from the weld metal (WM) through the heat-affected zone (HAZ) microstructures to the parent metal (PM).

The weld metal (WM) consists of columnar dendrites with a bainite microstructure. Some individual martensitic grains are also present in the middle of the deposited weld metal. The microstructure of the HAZ consists of martensite and bainite with a transition to the unaffected tempered martensitic microstructure of the parent metal (PM) (**Figures 8** and **9**).

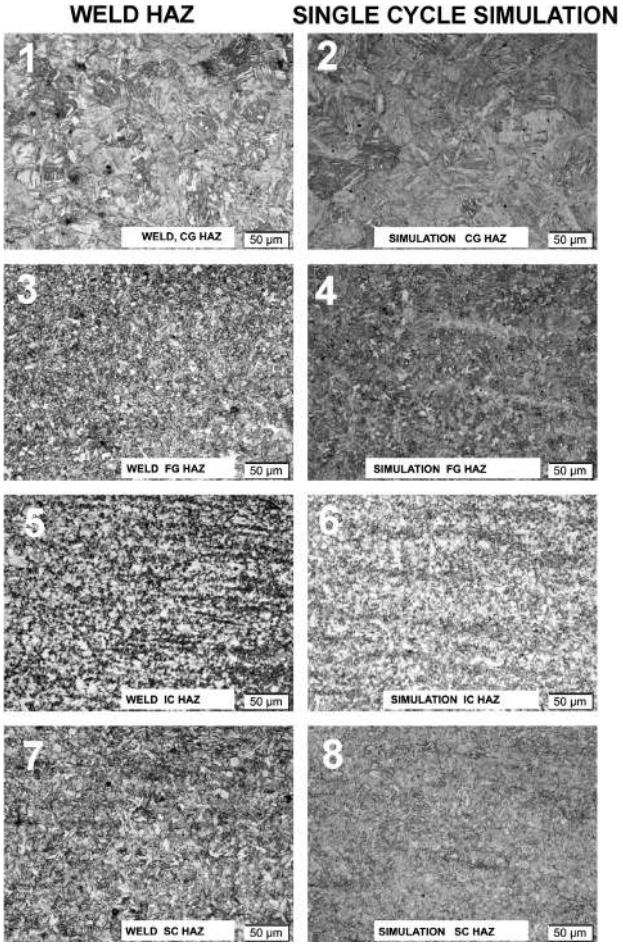

Figure 8: Real and simulated HAZ microstructures
Slika 8: Realne in simulirane mikrostrukture TVP

Figure 8.1 shows the coarse grains (CGs) that are present in the HAZ adjacent to the fusion boundary of the weld. The fine-grain (**FG**, **Figure 8.3**) region follows due to the peak temperature above A_{C3} but lower than in the CG region, the temperature and time were not sufficient to cause severe grain growth. With increasing distance from the fusion boundary there are inter-critical (**IC, Figure 8.5**) and subcritical (**SC, Figure 8.7**) regions of the HAZ.

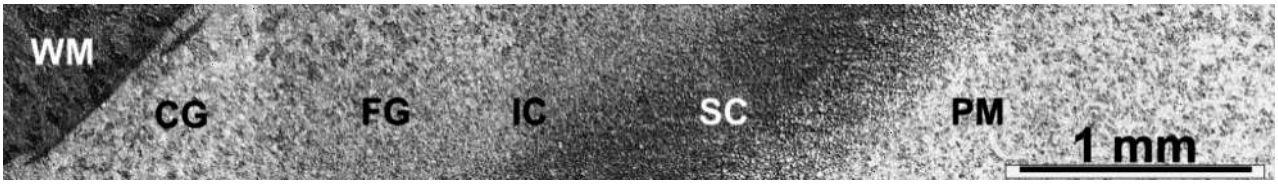

Figure 7: Transition from weld metal (WM) to parent metal (PM)
Slika 7: Prehod iz vara (WM) v osnovni material (PM)

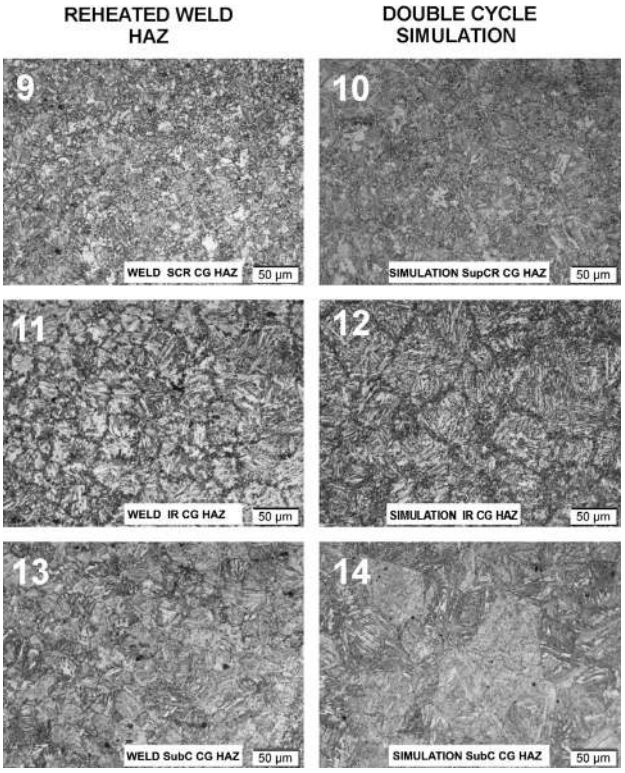

Figure 9: Real and simulated HAZ microstructures; reheated regions
Slika 9: Realne in simulirane mikrostrukture TVP; ponovno pregreta področja

The reheated inter-critical region (**Figure 9.11** and **9.12**) is very susceptible to failure, due to the fact that the phase transformation into austenite began on the grain boundaries; these small areas were then quickly cooled and are in turn hard and brittle. The subcritical regions are mainly tempered bainite and martensite with precipitated carbides and therefore represent no danger to the structural integrity of the weld. The simulated microstructures in **Figure 8** and **Figure 9** are labelled with even numbers. Although the grain size of the simulated specimen is slightly larger than that of the real welded joint when comparing the identical thermal cycle, we can distinguish a similarity between the welded HAZ and the dilatometer-simulated microstructures. The reason for the larger grains is that the thermal pinning is not considered in the thermal cycle simulation process.[6]

4 CONCLUSIONS

Normally, a dilatometer is used to observe a specimen's dimensional changes under a controlled heating or cooling rate. It can also be used to construct a continuous-cooling- transformation (CCT) diagram or an isothermal time-temperature-transformation (TTT) diagram. The TA DIL805A/D dilatometer with controlled heating and cooling fixtures was tested to simulate a real weld's HAZ microstructure. Based on the investigation the following can be concluded:

- The use of a simulated HAZ microstructure is a convenient way to study the weldability of a given steel.
- The presented investigation was limited to microstructure, due to the specimen's size and geometry.
- The simulation of a weld's HAZ microstructure is possible within the limits of the dilatometer's capabilities and the specimen's size.
- Hollow cylinder samples had a better response to the heating and cooling rate change than a solid cylinder.
- The inter-critical temperature during welding of S690QL is between 830 °C and 885 °C.

Acknowledgment

The authors are thankful to the Acroni d.o.o. and Elektrode Jesenice for the technical support related to work presented in this paper.

5 REFERENCES

[1] F. J. Winsor, ASM Handbook, Vol. 6: Welding, Brazing and Soldering, ASM, International, Materials Park, OH 1993, 662
[2] SIST EN 10025-6:2005+A1:2009, Hot rolled products of structural steels – Part 6: Technical delivery conditions for flat products of high yield strength structural steels in the quenched and tempered condition
[3] S. Kou, Welding metallurgy, 2nd ed., Wiley Interscience, Hooboken 2003, 406
[4] M. Hamada, Control of strength and toughness at the heat affected zone, Welding International, 17 (**2003**) 4, 265-270
[5] T. Lolla, S. S. Babu, S. Lalam, M. Manohar: Understanding the Role of Initial Microstructure on Intercritically Reheated Heat- Affected Zone Microstructures and Properties of Microalloyed Steels, Proc. of the 9th Inter. Conf., June 4–8, 2012 Chicago, 34-42
[6] Y. Shi, Z. Han, Effect of weld thermal cycle on microstructure and fracture toughness of simulated heat-affected zone for a 800 MPa grade high strenght low alloy steel, Journal of Materials Processing Technology, 207 (**2008**), 30–39, doi: 10.1016/j.jmatprotec.2007.12.049
[7] G. R. Goodall, J. Gianetto, J. Bowker, M. Brochu, Thermal simulation of HAZ regions in modern high strength steel, Canadian Metallurgical Quarterly, 51 (**2012**), 1, 58–66, doi:10.1179/1879139511Y.0000000023
[8] I. Samardžić, A. Stoić, D. Kozak, I. Kladaric, M. Dunđer, Application of Weld Thermal Cycle Simulator in Manufacturing Engineering, Journal of Manufacturing and Industrial Engineering, Journal of Manufacturing and Industrial Engineering, 12 (**2013**), 1–2, 7–11, doi: http://dx.doi.org/10.12776/mie.v12i1-2.177
[9] [9]G. L. Liang, S.W. Yang, H. B. Wu, X. L. Liu, Microstructure and mechanical performances of CGHAZ for oil tank steel during high heat input welding, Rare Metals 32 (**2013**) 2, 129–133, doi:10.1007/s12598-013-0036-y
[10] Y. Adonyi, Heat-Affected Zone Characterization by Physical Simulations, Welding Journal, 10 (**2006**), 42-47
[11] J. Wang, S. Lu, L. Rong, D. Li, Thermal cycling, microstructure and mechanical properties of 9Cr2WVTa steel welds, Journal of Materials Processing Technology, 222 (**2015**) 8, 434–443, doi:10.1016/j.jmatprotec.2015.03.017
[12] M. Dunđer, I. Samardžić, T. Vuherer, Dependence of hardness and impact energy on cooling time $\Delta t_{8/5}$ and temperature for S960QL, Metalurgija, 54 (**2015**) 3, 539–542, doi:10.12776/mie.v12i1-2.177
[13] Welding – Recommendations for welding of metallic materials – EN 1011-2 Part 2: Arc welding of ferritic steels

[14] I. Hajro, O. Pašić, Z. Burzić, Karakterizacija zavarenih spojeva na visokočvrstom konstrukcionom čeliku S690QL, Zavarivanje i zavarene konstrukcije, 58 (**2010**) 4, 123–129

[15] M. Shome, Effect of heat-input on austenite grain size in the heat affected zone of HSLA-100 steel, Materials Science and Engineering A, 39 (**2007**) 13, 454–460, doi:10.1016/j.msea.2006.09.085

[16] Acroni Micral 690 Datasheet, https://www.metalandsteel.com/documentserver/store/17606/2b66fa1b-adaa-4b42-9700- 1ab07d115e60.pdf

[17] SIST EN ISO 16834: – Welding consumables – Wire electrodes, wires, rods and deposits for gas shielded metal arc welding of high strength steels – Classification

[18] SIST EN ISO 15614-1: Specification and Qualification of Welding Procedures for Metallic Materials – Welding Procedure Test – Part 1: Arc and Gas Welding of Steels and Arc Welding of Nickel and Nickel Alloys

[19] R. Celin, J. Bernetič, D. A. Skobir Balantič, Welding of the steel gradeS890QL, Mater. Tehnol., 48 (**2014**) 6, 931–935

[20] S. Kožuh, M. Gojić, I. Ivanić, B. Kosec, Microstructure of welded austenitic stainless steel after annealing at 900 °C, Zavarivanje i zavarene konstrukcije, 61 (**2013**) 4, 149–156

[21] F. Tehovnik, B. Arzenšek, B. Arh, D. Skobir, B. Pirnar, B. Žužek, Microstructure evolution in SAF 2507 super duplex stainless steel, Mater. Tehnol., 45 (**2011**) 4, 339–345

[22] M. Pournavari, S. P. H. Marashi, H. L. Jaber, DP780 dual-phase-steel spot welds: critical fusion-zone size ensuring the pull-out failure mode, Mater. Tehnol., 49 (**2015**) 4, 579–585, doi:10.17222/mit.2014.184